International Journal of Heat and Mass Transfer 52 (2009) 5167–5172

Contents lists available at ScienceDirect

International Journal of Heat and Mass Transfer

journal homepage: www.elsevier.com/locate/ijhmt

Formation and sublimation of ice structures over cylindrical collectors

Guillermo G. Aguirre Varela, Nesvit E. Castellano, Eldo E. Ávila *

Facultad de Matemática Astronomía y Física, Universidad Nacional de Córdoba, CONICET, Ciudad Universitaria, 5000 Córdoba, Argentina

ARTICLE INFO

Article history:
Received 10 October 2008
Received in revised form 14 April 2009
Available online 12 June 2009

Keywords:
Ice sublimation
Ice accretion
Lobe's structure
Ice morphology

ABSTRACT

A series of experiments were conducted for temperatures below 0 °C, air velocities of 5, 8 and 11 m s^{-1}, with the goal of studying the structural characteristics and sublimation of ice structures grown over cylindrical rotating collectors. The results show that the accreted ice presents structures similar to lobes. A connection between the surface characteristics of the accretion and the environmental conditions was established. It was also found that the size and lobe-number density of the ice accreted on the surface do not affect sublimation rate when the sublimation process occurs in free convection conditions.

1. Introduction

A cloud or fog consists of small water droplets or ice crystals. Even if the temperature is below the freezing point of water, the droplets may remain in the liquid state. Such supercooled droplets freeze immediately upon impact with objects in the airflow. This process is usually called accretion. When the temperature of the flux of water droplets towards the object is below the freezing point of water, and each droplet freezes before the next droplet impinges on the same spot, the ice growth is said to be dry. When the water flux increases, the ice growth will tend to be wet, because the droplets do not have the necessary time to freeze, before the next one impinges.

Atmospheric icing of structures, trees, power line cables, road surface, etc. has been the subject of several physical and engineering studies for decades, specially focusing on learning about the accretion process in order to reduce problems and economical loss caused by this phenomenon.

Numerous numerical models have been developed with the purpose of understanding and determining the ice accretion process as well as the structure and morphology of the accreted ice on collectors of different geometries [1–3]. Usually, numerical models require empirical adjustment of parameters such as ice density, temperature of the accretion and heat and mass transfer coefficients [4–7].

The physical properties and the appearance of the accreted ice will vary widely according to meteorological conditions during ice growth. Basically, they depend on the shape and size of the collector (a), the wind speed (V), the air temperature (T), the collector temperature (T_s), the liquid water content (LWC), the droplet size distribution, and the accreted ice density (ρ). Some of these variables are measured directly in the experiments while others need to be determined indirectly by means of other parameters.

The temperature of the collector can be significantly increased by the releasing of the latent heat of fusion as the supercooled water droplets freeze on its surface. This temperature is one of the most important variables involved in the accretion process because it controls the density of the accretion and in consequence it affects the surface characteristics and the appearance that accreted ice achieves. The temperature of the accreted ice is determined by the balance between the rate at which latent heat is released by the freezing of collected water drops and the rate at which heat can be lost by convection and sublimation, i.e. the heat and mass transfer process plays an essential role in the temperature of the accretion. To calculate this temperature it is necessary to introduce parameterizations of the Nusselt number (Nu) and the Sherwood number (Sh), which are dimensionless numbers related to the heat and mass transfer coefficients, respectively [8].

There is experimental evidence [5,7,9,10,15] that the roughness of the accretion affects the air flux in its vicinity and therefore the heat transfer process (Nu). Therefore, the following questions are in order: (1) How are these rough surfaces generated? (2) How is the mass transfer between the accretion and the surroundings when the surface of the sublimating ice is not smooth but rough? In order to provide information regarding these questions, the present work presents studies of ice accretions, together with measurements of their sublimation rate, i.e. mass sublimating from the deposit per unit time. This work also focuses on the structural characteristics of the growing surface. The results presented correspond to three different air-flux velocities for the accretion growth.

* Corresponding author.
E-mail address: avila@famaf.unc.edu.ar (E.E. Ávila).

0017-9310/$ - see front matter © 2009 Elsevier Ltd. All rights reserved.
doi:10.1016/j.ijheatmasstransfer.2009.05.002

Nomenclature

a_{max}	diameter of the ice-covered cylinder (mm)
d_m	median diameter of the spectra of cloud droplet (μm)
Dm	mean diameter of the lobes (mm)
Ew	effective liquid water content (g m^{-3})
K	Stokes' number
L	length of the ice-covered cylinder (mm)
MAR	mass accretion rate (g s^{-1} m^{-2})
t	total time of the accretion process (min)
T	air temperature (°C)
T_s	accretion surface temperature (°C)
V	wind speed (m s^{-1})
V_e	impact velocity at the stagnation point of the cylinder (m s^{-1})
X	Macklińs parameter (μm m s^{-1}°C^{-1})
Greeks	
α	sublimation rate (g s^{-1} m^{-2})
η	surface lobe density (mm^{-2})
η_a	dynamic viscosity of air (kg m^{-1} s^{-1})
ρ	accreted ice density (g cm^{-3})
ρ_a	air density (g cm^{-3})
ρ_w	water density (g cm^{-3})

2. Experimental setup

Ice structures were formed over a cylindrical collector placed inside a cold chamber of height 3 m and floor area 2 × 3 m^2 and of controlled temperatures ranging from 0 to –30 °C. A vertical upward-flux wind tunnel was mounted inside the chamber. Fig. 1 shows a schematic diagram of the wind tunnel and other devices used in the experiments. A cylindrical rod of diameter a = 4 mm was placed in the wind tunnel and connected to a controlled frequency rotation device which allows the rod rotates around its axis (0.5 Hz was used in this study). This device allows the whole cylindrical rod to be accreted and azimuthally symmetric ice deposits were obtained.

The cylinder was placed with its axis orthogonal to the air flowing in the tunnel. A water drop generator was placed at the entrance of the tunnel, which provided the cloud of water drops necessary to produce accretion on the cylinder. The speed of the airflow past the collector (V) was controlled by adjusting the power to an air pump and was determined by using a Pitot-tube type anemometer. The measurements were conducted for air velocities of 5, 8 and 11 m s^{-1} determined with an error of ±0.5 m s^{-1}.

The water droplet sizes were obtained by taking cloud samples with a microscope glass-slide covered with a thin film of 5% formvar solution. Several cloud samples were taken at the position of the collector for different velocities. The samples were analyzed under a microscope, and the droplet sizes were determined. The median diameter (d_m) of the spectra determined was 30, 31 and 30 μm, for V = 5, 8 and 11 m/s, respectively. The range of sizes reached 80 μm, and in some cases, drops were found with sizes as large as 100 μm. Fig. 2 is an example of a typical size-distribution histogram, obtained for an experiment corresponding to 5 m/s.

Besides d_m, clouds were also characterized by the effective liquid water content, Ew. This variable represents the amount of liquid water, per unit air volume, which can be collected by the target, $Ew = M/AVt$, where M is the mass of water deposited, A is the effective cross-section in the air flux, V is the air-flux velocity and t is the accretion time. The effective liquid water content

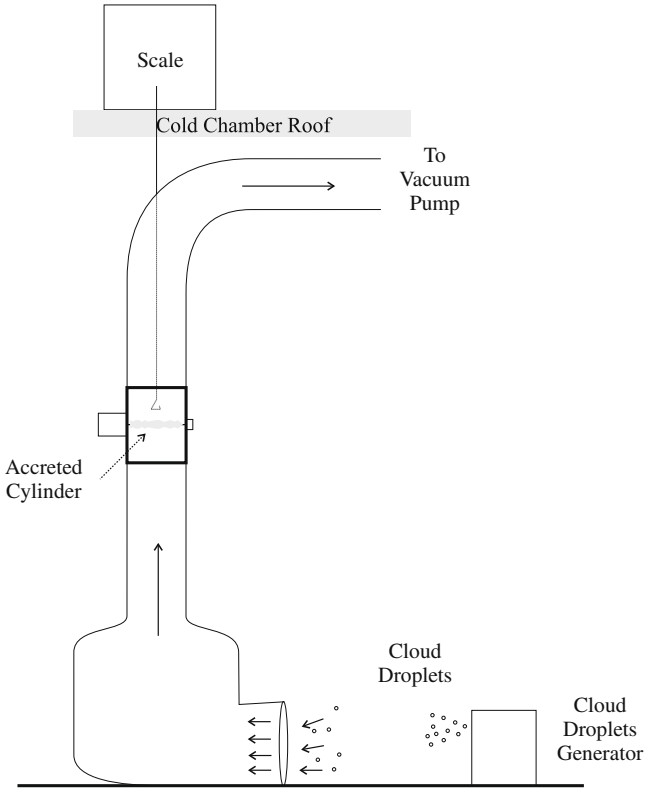

Fig. 1. Sketch of the experimental device used for the laboratory study.

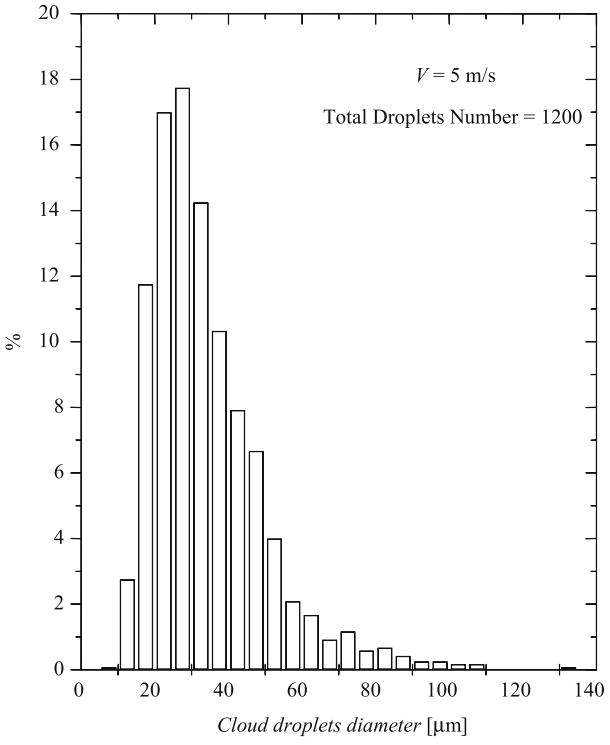

Fig. 2. Cloud droplets size distribution used in the experiments.

(*Ew*) is usually smaller than the liquid water content (*LWC*) which represents the total mass of the cloud water droplets per unit volume. *Ew* was determined using dimensions obtained through photographs of the accretions. Section *A* was determined as the average between the area of the ice-free cylinder and that of the ice-covered cylinder at the end of the experience. Accretions were carried out for times ranging from 14 to 28 min. During this time, velocity *V*, the amount of water in the cloud, and room (ambient) temperature were all held constant.

Once the ice accretion was obtained, air flux was interrupted, and the collector removed from the rotating system and held from a scale, allowing the determination of mass as a function of time. Values for the mass of the accretion were recorded in a computer until the ice completely sublimated. The appreciation of the scale used to register masses was 10^{-5} g.

While measurements were carried out, relative humidity inside the chamber varied between 70% and 80%. The size of the deposit (diameter a_{max} and length L) and its surface characteristics were obtained through photographs taken immediately after accretion and when the ice-covered cylinder was hung on the scale. The photographs in Fig. 3 are examples of the ice structures obtained through accretion, a_{max} and L are indicated in the figure. The values of a_{max} and L were obtained averaging different measurements made on several of the pictures taken. The parameters used in each experiment are shown in Table 1, where T is the temperature of the chamber during sublimation, *MAR* is the mass accretion rate per unit surface area ($MAR = V\,Ew$), and t is the total time of the accretion process.

3. Results and comments

3.1. Accretion morphology

As can be seen from Fig. 3, accretion surface presents structures similar to lobes. Lobe distribution and sizes changed for each accretion. In order to characterize the form of the accretions, the diameter of a circle with an area equivalent to the base of the lobe was determined and for each accretion the distribution of these diameters was obtained. The mean diameter (*Dm*) was then obtained for each distribution and this value was taken as an estimate of the size of the lobes in each accretion. Accretion surfaces were further characterized by the surface lobe density (η), defined as the number of lobes per unit cylinder area. The density of the ice structure (ρ) was characterized by the mass and volume of the accretion; the last parameter was determined from dimensions measured through photographs.

The characteristics of the accretions are determined by microphysical processes but are probably not completely determined by the environmental conditions (T, V, *Ew* and d_m) used in each experiment. However, based on inspection of the photographs of all the experiments, support was found to assume that the general surface characteristics of the accretions (*Dm* and η) could be related to the environmental variables.

With the purpose of establishing a connection between the surface characteristics of the accretion and the sizes of the accretion as well as the environmental conditions, the Stokes' number (K) was used in data analysis. The Stokes' number is defined as

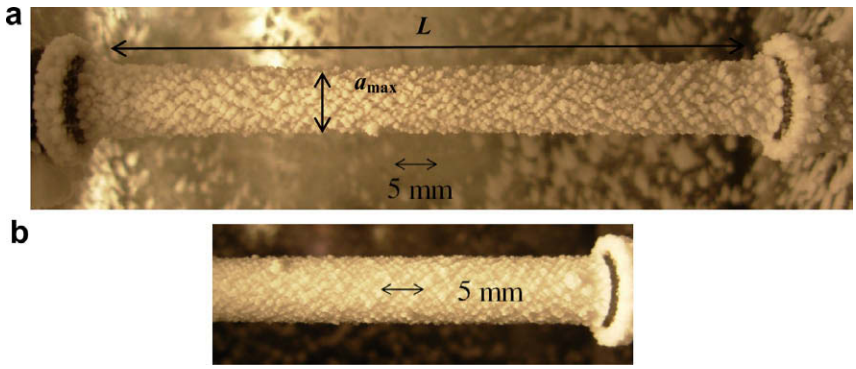

Fig. 3. Photographs of the ice structures obtained in the experiments. $Ta = -11$ °C, $d_m = 30$ μm. (a) $V = 5$ m/s and (b) $V = 11$ m/s.

Table 1
Experimental conditions (V, T, d_m, *Ew*), time of the accretion (t), dimensions of the accretion (a_{max} and L) and the mass accretion rate (*MAR*) corresponding to each experiment.

No.	T (°C)	V (m/s)	d_m (μm)	t (min)	L (mm)	a_{max} (mm)	Ew (g m^{-3})	MAR (g s^{-1} m^{-2})
1	−11 ± 1	5.0 ± 0.5	30 ± 1	14.0 ± 0.2	72.0 ± 0.1	7.2 ± 0.2	0.24 ± 0.06	1.20 ± 0.60
2	−11 ± 1	5.0 ± 0.5	30 ± 1	14.0 ± 0.2	78.9 ± 0.3	8.4 ± 0.2	0.27 ± 0.06	1.35 ± 0.60
3	−11 ± 1	5.0 ± 0.5	30 ± 1	28.0 ± 0.2	71.0 ± 0.6	8.6 ± 0.2	0.19 ± 0.04	0.95 ± 0.50
4	−11 ± 1	5.0 ± 0.5	30 ± 1	28.0 ± 0.2	66.6 ± 0.3	5.7 ± 0.2	0.08 ± 0.02	0.40 ± 0.50
5	−11 ± 1	8.0 ± 0.5	31 ± 1	28.0 ± 0.2	68.4 ± 0.1	6.4 ± 0.1	0.14 ± 0.02	1.12 ± 0.50
6	−11 ± 1	8.0 ± 0.5	31 ± 1	28.0 ± 0.2	68.4 ± 0.1	7.2 ± 0.1	0.16 ± 0.02	1.28 ± 0.50
7	−11 ± 1	11.0 ± 0.5	30 ± 1	14.0 ± 0.2	68.8 ± 0.1	8.6 ± 0.1	0.49 ± 0.05	5.39 ± 0.60
8	−11 ± 1	11.0 ± 0.5	30 ± 1	14.0 ± 0.2	69.4 ± 0.1	9.2 ± 0.2	0.60 ± 0.07	6.60 ± 0.60
9	−11 ± 1	11.0 ± 0.5	30 ± 1	14.0 ± 0.2	68.6 ± 0.1	7.3 ± 0.1	0.36 ± 0.04	3.96 ± 0.50
10	−11 ± 1	11.0 ± 0.5	30 ± 1	14.0 ± 0.2	68.8 ± 0.2	7.3 ± 0.2	0.61 ± 0.07	6.71 ± 0.60
11	−11 ± 1	11.0 ± 0.5	30 ± 1	28.0 ± 0.2	68.7 ± 0.1	7.3 ± 0.2	0.18 ± 0.02	1.98 ± 0.50
12	−5 ± 1	5.0 ± 0.5	30 ± 1	28.0 ± 0.2	67.5 ± 0.1	6.9 ± 0.1	0.21 ± 0.05	1.05 ± 0.60
13	−5 ± 1	5.0 ± 0.5	30 ± 1	28.0 ± 0.2	67.5 ± 0.3	5.8 ± 0.1	0.11 ± 0.02	0.55 ± 0.50
14	−5 ± 1	8.0 ± 0.5	31 ± 1	14.0 ± 0.2	69.1 ± 0.1	8.7 ± 0.2	0.61 ± 0.09	4.88 ± 0.60
15	−5 ± 1	11.0 ± 0.5	30 ± 1	14.0 ± 90.2	69.0 ± 0.1	9.0 ± 0.1	0.68 ± 0.07	7.48 ± 0.60

$K = \rho_w d_m^2 V / 9\eta_a a_{max}$, where ρ_w is water density, and η_a the dynamic viscosity of air. The number K is related to water drop collection efficiency and serves to describe how well drops follow the flow current lines of the wind field around the collector [11,12].

After trying several combinations of the variables we found that a suitable parameter to characterize the surface characteristics of the accretion is $Ew\ K^{-1}$. It is important to recall that Ew is one of the variables that handles the temperature that ice accretion can achieve. This temperature is a key variable to determine the surface characteristics of the accretion. The average size of the lobes is expected to be proportional to Ew and their density to be inversely proportional to this variable. On the other hand, the Stokes' number is proportional to water drop collection efficiency and it is expected that small droplets or low velocities (low K values) form smaller and denser lobes on the surface accretion than those produced by larger K values. For these reasons, it seems reasonable to parameterize the surface characteristic of the accretion by $Ew\ K^{-1}$.

Fig. 4 displays the experimental values of Dm and η as a function of the dimensionless parameter $Ew\ \rho_a{}^{-1}K^{-1}$. The air density (ρ_a) was included in the parameter in order to make it dimensionless. As can be seen, the results show that the size and density of the lobes increase exponentially with $Ew\ \rho_a{}^{-1}K^{-1}$. Thus, they can be parameterized as

$$Log\, Dm = 0.0385 Ew\, \rho_a^{-1} K^{-1} - 0.333 \quad (1)$$

$$Log\, \eta = -0.0642 Ew\, \rho_a^{-1} K^{-1} + 0.4 \quad (2)$$

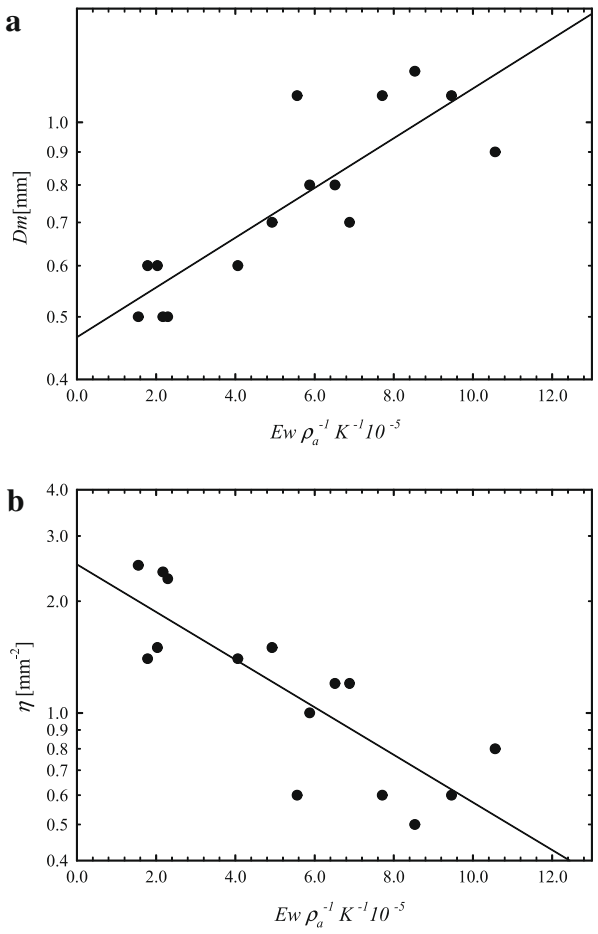

Fig. 4. (a) Mean lobe diameter (Dm) and (b) surface lobe density (η) as a function of the dimensionless parameter $Ew\ \rho_a{}^{-1}K^{-1}$.

The size (Dm) and density (η) of the lobes are given in mm and mm^{-2}, respectively. It is important to note that the number of experimental data is limited and the values span only a single decade; therefore, the semi-log relationships proposed here need to be considered carefully and in the context of the range of variation of the variables.

Since Dm and η seem to depend on the same variables, the question arises as to which is the relation between them. Fig. 5

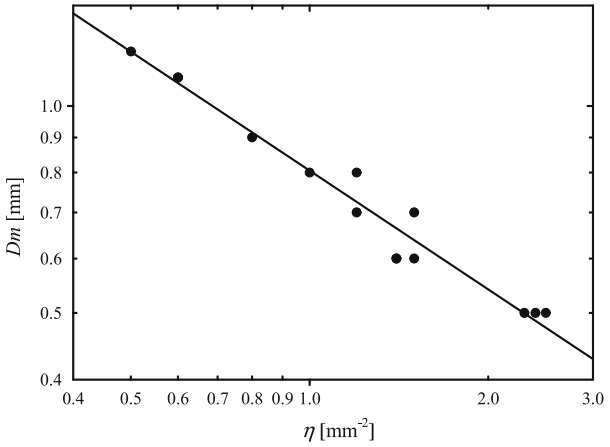

Fig. 5. Relationship between lobe diameter and density on the surface of cylinders.

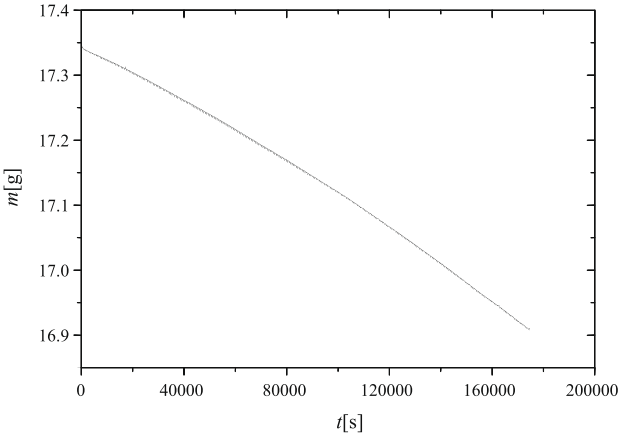

Fig. 6. Time evolution of the accreted ice mass in free convection.

Table 2
Experimental values of the sublimation rate (α) obtained, together with the corresponding Dm, η, ρ and temperature values.

No.	T_a (°C)	Dm (mm)	η (mm^{-2})	ρ ($g\,cm^{-3}$)	α ($\times 10^{-4}\ g\,s^{-1}\,m^{-2}$)
1	−11 ± 1	0.8 ± 0.2	1.0	0.20 ± 0.02	−1.8 ± 0.1
2	−11 ± 1	1.1 ± 0.3	0.6	0.16 ± 0.02	−6.2 ± 2.0
3	−11 ± 1	1.1 ± 0.3	0.6	0.22 ± 0.02	−1.9 ± 0.1
4	−11 ± 1	0.5 ± 0.1	2.5	0.21 ± 0.04	−18.0 ± 5.0
5	−11 ± 1	0.6 ± 0.2	1.4	0.50 ± 0.03	−16.0 ± 0.8
6	−11 ± 1	0.5 ± 0.2	2.3	0.43 ± 0.03	−1.3 ± 0.6
7	−11 ± 1	0.8 ± 0.3	1.2	0.57 ± 0.03	−13.4 ± 1.6
8	−11 ± 1	1.2 ± 0.4	0.5	0.61 ± 0.05	−40 ± 10
9	−11 ± 1	0.6 ± 0.2	1.4	0.57 ± 0.03	−13.3 ± 1.3
10	−11 ± 1	0.7 ± 0.2	1.2	0.97 ± 0.08	−5.8 ± 0.7
11	−11 ± 1	0.6 ± 0.2	1.5	0.59 ± 0.07	−15.9 ± 0.8
12	−5 ± 1	0.7 ± 0.2	1.5	0.39 ± 0.02	−4.4 ± 0.3
13	−5 ± 1	0.5 ± 0.1	2.4	0.32 ± 0.02	−10.6 ± 1.6
14	−5 ± 1	0.9 ± 0.2	0.8	0.52 ± 0.06	−10.1 ± 0.6
15	−5 ± 1	1.1 ± 0.3	0.6	0.72 ± 0.03	−16.9 ± 1.0

shows values of Dm vs η. It is possible to observe how lobe size decreases as lobe density increases. This is in agreement with the idea that a high small-size lobe density should correspond to a smooth surface. This figure shows the close relationship between lobe diameter and density on the surface of cylinders, as expressed by the linear fit shown in the plot. From this plot the dependence of Dm on η is

$$Dm = 1.24\eta^{-0.58} \tag{3}$$

where Dm and η are given in mm and mm^{-2}, respectively.

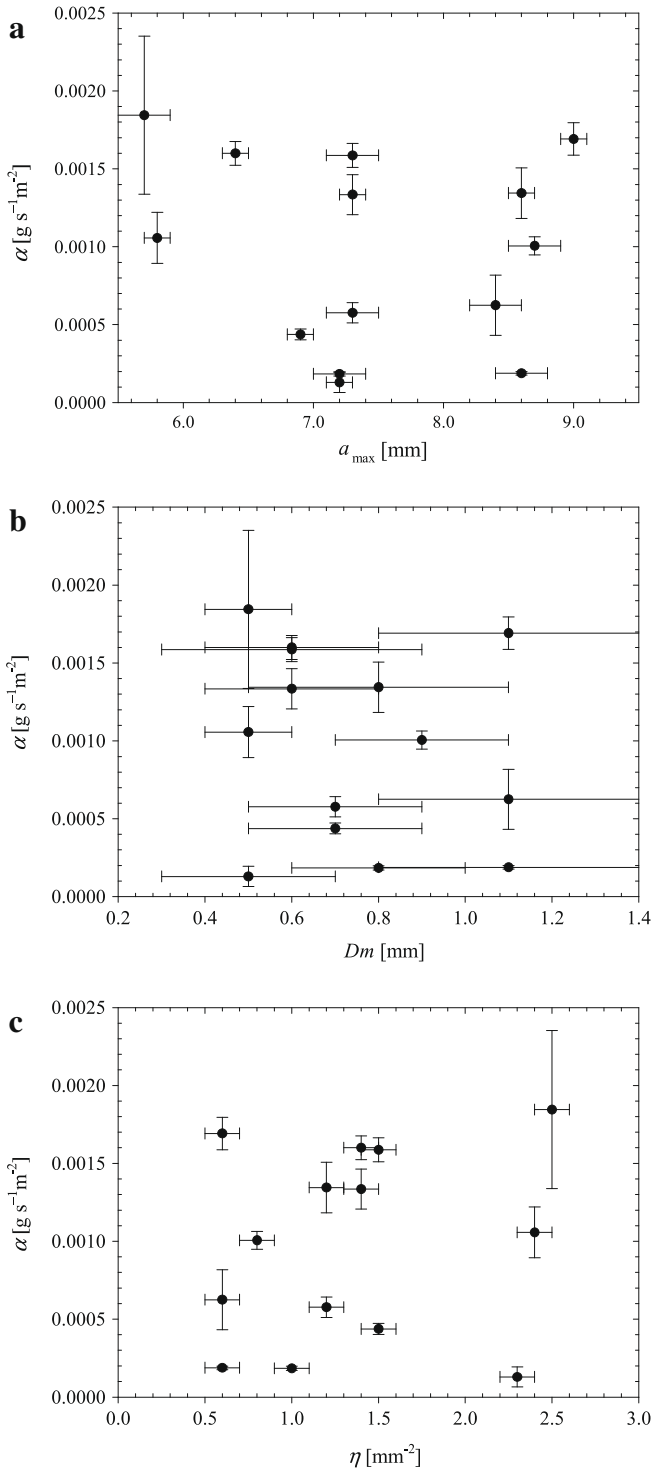

Fig. 7. Sublimation rate values as a function of (a) a_{max}, (b) Dm and (c) η.

The density of the accretion is determined by the tendency of the colliding supercooled water droplets to spread out on the surface, as well as by the speed of the freezing process. When the droplet tends to maintain its shape during the freezing process, the accretion builds with higher surface roughness and a more porous structure. The values of mean ice density obtained (ρ) were calculated by using the empirical fit given by Macklin [13]: $\rho = 0.11X^{0.76}$, where X is defined as $X = d_m V_e/2T_s$, and V_e is the impact velocity of the droplet at the stagnation point of the cylinder and T_s the accretion surface temperature. Because of the droplet inertia and the change in droplet trajectory, the impact velocity at the stagnation point (V_e) is smaller than the airflow velocity (V), and it was calculated following Castellano et al. [6]. The temperature of the accretion (T_s) was obtained according to Ávila et al. [5]. In general, the experimental data obtained in the current work are within the dispersion of the data obtained by Macklin [13]. By analyzing the ice density values as a function of the parameters characterizing the morphology of the accretion, Dm and η, it was possible to conclude that there is not any relationship between them.

3.2. Accretion sublimation

Fig. 6 is a typical curve showing the evolution of an accreted ice mass as a function of time, when hanging from the scale, free of wind and cloud. In order to perform an analysis of the data, the sublimation rate α was defined as accretion mass variation per unit time and surface area, $\alpha = \Delta m/A\Delta t$. This figure shows that the sublimation rate is slowly modified over a long period; for this reason the value of α was determined by using the first 10^4 s in each experiment. Table 2 displays values of α obtained, together with the corresponding Dm and η values, as well as the values of temperature and ρ.

In order to check whether the sublimation rate is related to the morphology of the accretion, Fig. 7a, b and c present results for α as a function of a_{max}, Dm and η, respectively. The plots clearly show that α is not related to either of these variables, characterizing accretion surface roughness.

This finding is consistent with the results by Aguirre Varela et al. [14], who studied the influence of lobes on the heat transfer process to the environment. They used metallic cylinders, the surfaces of which were molded using different numbers of lobes and lobes of different heights. They found that the presence of lobes on the surface did not significantly modify the ventilation coefficient of the cylinders. It is important to remark that the mechanisms of heat and mass transfer in ice are analogous.

4. Conclusions

The current work presents an experimental study of the surface characteristics of the ice accretion on a rotating cylindrical collector. The presence of lobes was observed on the collector; the surface characteristics of the accretion depend on the Stokes' number as well as the environmental conditions used in the experiments. A marked correlation was also found between the average lobe diameter and lobe surface density. These irregularities on the accreted surface, however, do not affect its sublimation rate when the sublimation process occurs by free convection. According to the results obtained, in the case of free convection, ice structures with smooth surface or with protuberances sublimate in the same manner, which leads to believe that the boundary air layer surrounding the ice surface smoothens the presence of lobes.

These new results are a contribution to the accretion processes occurring in cold regions.

Acknowledgments

This work was supported by Secretaría de Ciencia y Tecnología de la Universidad Nacional de Córdoba, Consejo Nacional de Investigaciones Científicas y Tecnológicas (CONICET), and Agencia Nacional de Promoción Científica (FONCYT). We want to thank José Barcelona and Rodrigo Bürgesser for their technical assistance.

References

[1] T.W. Brakel, J.P.F. Charpin, T.G. Myers, One-dimensional ice growth due to incoming supercooled droplets impacting on a thin conducting substrate, Int. J. Heat Mass Transfer 50 (9–10) (2007) 1694–1705.
[2] Fu Ping, M. Farzaneh, G. Bouchard, Two-dimensional modeling of the ice accretion process on transmission line wires and conductors, Cold Regions Sci. Technol. 46 (2) (2006) 132–146.
[3] L. Makkonen, M.M. Oleskiw, Small-scale experiments on rime icing, Cold Regions Sci. Technol. 25 (3) (1997) 173–182.
[4] O.B. Nasello, N.E. Castellano, On the search for a representative drag coefficient law to be used in hail trajectory simulations, Atmos. Res. 47 (47-48) (1998) 4887–4896.
[5] E.E. Avila, N.E. Castellano, C.P.R. Saunders, Effect of cloud droplet spectra on the average surface temperature of ice accreted on fixed cylindrical collectors, Quart. J. Roy. Meteorol. Soc. 125 (555) (1999) 1059–1074.
[6] N.E. Castellano, O.B. Nasello, L. Levi, Study of hail density parameterizations, Quart. J. Roy. Meteorol. Soc. 128 (583) (2002) 1445–1460.
[7] G.G. Aguirre Varela, N.E. Castellano, E.E. Avila, Comment on the porosity effect of ice accretions on the heat transfer coefficient, Quart. J. Roy. Meteorol. Soc. 131 (605) (2005) 97–99.
[8] F. Incropera, D. De Witt, Introduction to Heat Transfer, third ed., Wiley, New York, 1996.
[9] N.E. Castellano, E.E. Avila, C.P.R. Saunders, Dependence of the average surface temperature on cloud droplet spectra for rime ice accreted on fixed spherical collectors, J. Geophys. Res.-Atmos. 104 (22) (1999) 27399–27406.
[10] G.G. Aguirre Varela, N.E. Castellano, E.E. Avila, Effect of internal flux on the heat transfer coefficient in circular cylinders in cross flow, Int. J. Heat Mass Transfer 50 (19–20) (2007) 4098–4104.
[11] I. Langmuir, K.B. Blodgget, Mathematical investigation of water droplet trajectories, Program Press 196, vol. 10, Tech. Report No. RL-224, US Air Force, DC, 1945.
[12] K. Finstand, E. Lozowski, E. Gates, A computational investigation of water droplet trajectories, J. Atmos. Ocean. Technol. 5 (1) (1988) 160–170.
[13] W.C. Macklin, The density and structure of ice formed by accretion, Quart. J. Roy. Meteorol. Soc. 88 (375) (1962) 30–50.
[14] G.G. Aguirre Varela, N.E. Castellano, R.G. Pereyra, E.E. Avila, The effect of surface lobes on heat transfer from an ice particle, Quart. J. Roy. Meteorol. Soc. 129 (595) (2003) 3425–3438.
[15] E.E. Avila, R.G. Pereyra, N.E. Castellano, C.P.R. Saunders, Ventilation coefficients for cylindrical collectors growing by riming as a function of the cloud droplet spectra, Atmos. Res. 57 (2) (2001) 139–150.